

53rd CIRP Conference on Manufacturing Systems

# Digital Process Management for the Integrated Bending of Thermoplastic CFRP Tapes

Daniel Kupzik\*, Junsheng Ding, Sven Coutandin, Jürgen Fleischer

*wbk Institute of Production Science, Karlsruhe Institute of Technology (KIT), Kaiserstraße 12, 76131 Karlsruhe, Germany*

\* Corresponding author. Tel.: +49-1523-9502594; fax: +49-721-608-45005. E-mail address: [daniel.kupzik@kit.edu](mailto:daniel.kupzik@kit.edu)

## Abstract

A bending based approach for the preforming of carbon fiber reinforced thermoplastic (CFRTP) tapes has been implemented at wbk Institute of Production Science. In early experimentation, it became evident that the process requires regular adaption of process parameters in order to meet the desired quality level. To limit the manual effort, the parameter variation and process characterization should be automated. In this paper, an approach for the automatic parameter identification and tuning through systematic variation combined with optical process measurement is presented. The functionality of the measurement system as well as the parameter identification and error compensation are described.

© 2020 The Authors. Published by Elsevier B.V.

This is an open access article under the CC BY-NC-ND license (<http://creativecommons.org/licenses/by-nc-nd/4.0/>)

Peer-review under responsibility of the scientific committee of the 53rd CIRP Conference on Manufacturing Systems

*Keywords:* Fiber Reinforced Plastic; Optical Measurement; Process Control

## 1. Introduction

Thermoplastic unidirectional tape (UD-tape) is a high performance material type for structural components. It consists of continuous fibers embedded in a thermoplastic matrix. The fibers enable high strength and stiffness values in longitudinal direction while the matrix supports them against buckling and transverse loads. Possible applications are high pressure tubes or large structures. For the manufacturing of UD-tape structures, several processes are available. Tubes can be wound [1] while large structures are often laid by a special laying device [2]. Smaller structures can be produced using most of the common composite manufacturing processes like the combination of draping and molding [3]. Existing processes either require component specific tools for the forming [4, 5] of the tapes or offer only a low complexity of the geometry [6], thus causing high specific cost for low volume components. In the project GRK2078, UD-tapes are used as a local reinforcement in thermoplastic components. Therefore a novel process [7] for the bending based preforming of the line-like reinforcement structures is under development. The aim is a

near net-shape preform which is ready for co-molding with a liquefied thermoplastic mass. The process does not require component specific tooling and can be conducted while unreeling the tape, thus shortening the process chain. To use this simplification, two limitations have to be accepted. The process has different restrictions and abilities than most known processes and therefore requires an adapted variation of the near-net shape geometry. This is acceptable, as the manufactured preforms will be formed to their final shape during co-molding. Secondly, the tool-less bending of the tape in open space requires carefully chosen process parameters (e.g. temperatures and cooling duration). Choosing these parameters and keeping them updated to changing environmental conditions up to now required regular manual adaption. To overcome this disadvantage, a control loop for the parameter adaption is implemented.

For the parameter adaption, a stereo camera based measurement system is implemented for high-resolution shape measurement of the UD-tapes. This system can also be used for the compensation of systematic error. In the state of the art, optical measurement systems are widely used for the

deformation measurement [8, 9], 3D reconstruction of products [10], or monitoring the manufacturing processes [11]. All of these systems are adapted to their specific tasks. In this paper, it is shown, how a stereo camera system can be adapted to measure the position and amount of a bend in a UD-tape in a research environment.

## 2. Bending based forming

As it was desired to form the UD-tape without component specific tools, a new process had to be developed. The main demand of tool-less manufacturing is to control the deformation of the material. A possible strategy to reach this goal is to design the process in a way which makes it easy to control. This was done by limiting the forming to local bending of the tape. The deformation during bending was controlled by heating the tape only locally and thereby limiting the degrees of freedom within the forming process. With a stiff tape which is only softened along a line, deformations can solely occur in a way as if the two stiff ends of the tape were connected by a rotational hinge with its axis along the molten line. This movement can be kinematical described in an analytical model and controlled by a six-axis-robot. The process steps in a practical demonstrator cell are shown in Fig. 1 [12]. In the first step, tape is supplied to the bending area, gripped by the robot and clamped by the supply unit. In the second step, a line normal to the tape direction is heated. In the third step, it is bent. These three steps can be repeated until a complex shape of the tape is obtained. In the end, the preform will be separated from the supply by a cutting unit (step 4).

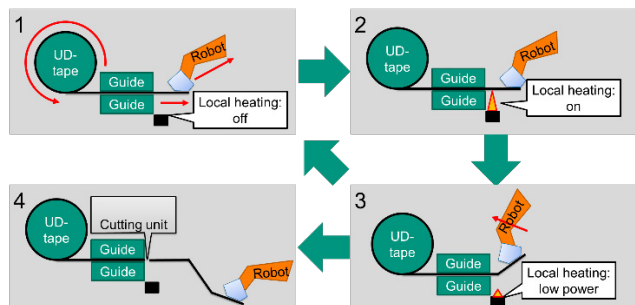


Fig. 1: Steps of the iterative bending process.

Possible tape geometries are shown in Fig. 2. Fig. 3 presents the kinematic description of a single bend consisting of the distance  $l$  between two bends, the skewness of the bending line  $\alpha$  and the amount of bending  $\beta$ .

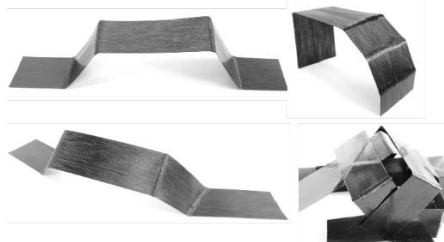


Fig. 2: Possible tape geometries of single tapes and a joined reinforcement.

As the material deformation is very local, the process will reliably deliver decent results if process parameters are chosen correctly and the material is sufficiently softened. In the

experimentation TenCate TC960 (carbon fibers with polypropylene matrix) was used.

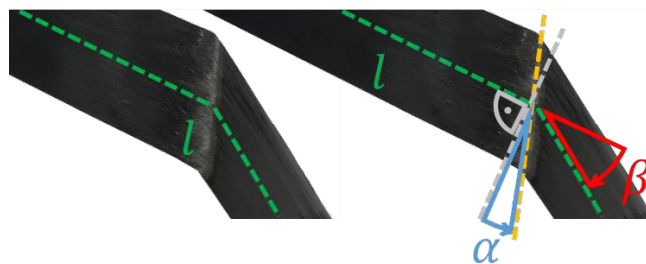


Fig. 3: Kinematic description of a single bend. Green line: middle axis of the tape; grey line: line normal to the middle axis,  $\alpha$ : rotation angle of the bending line, yellow line: bending line,  $\beta$ : bending angle,  $l$ : distance between two bends

The main components of the demonstrator cell for the bending process is shown in Fig. 4. It has a halogen lightbulb as heat source. The preheating time is defined as the time the heating is switched on before the robot is moving. The heating time is the heating duration while the robot is already moving.

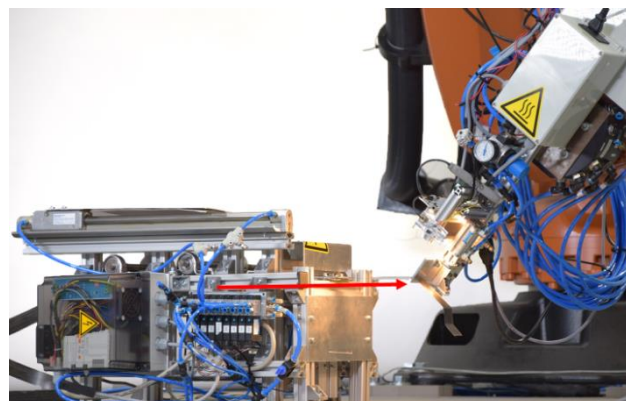


Fig. 4: Supply unit (left) and end-effector with activated halogen heating (right). The tape is pushed forward by a roller along the red arrow. The robot end-effector can then grip the tape, heat it and bend it.

The two main challenges in forming precise shapes are finding the correct bending movement and choosing the heating time. For the bending movement, a kinematic description of the robot movement was found. The required heating power is still challenging as it is depending on external influencing factors like the ambient temperature, movement of the air and the properties of the current tape batch. One example is that a certain minimum heating duration is necessary to fully melt the matrix in the desired patch area. Exemplary results for the resulting bending angle (desired angle  $\beta = -45^\circ$ ) depending on the overall heating time are shown in Table 1.

Table 1: example measurement of the influence of a parameter on the results:

Overall heating time	1.5 s	2.0 s	2.5 s	3.0 s	3.5 s	4.0 s	4.5 s	5.0 s
Bending angle $\beta$	0°	0°	-10°	-35°	-40°	-42°	-43°	-43°

Resulting from this, long-term reliable process parameters can only be chosen if high safety factors are accepted which slow the process down. To find the best compromise between manufacturing reliability and speed, the used process parameters should be adapted to the current process conditions

to keep the process time down to what is necessary at the time of manufacturing. The presented control loop (Section 4.1) will be used to conduct this adaption. It uses an optical measurement system to determine the current conditions and adjusts process parameters accordingly.

### 3. Digital process chain

The demonstrator cell is equipped with a mid-size industrial robot which is controlled by a python environment on a nearby computer. This setup was chosen to supply a flexible environment for research purposes. The computer calculates the desired tape geometry, controls the robot movement and can be used to execute further tasks like the measurement of the last manufactured bend. Currently, the workflow has the following steps:

- The computer calculates the desired tape geometry from a CAD file of the component region which shall be reinforced and saves it to a geometry-file [13].
- The computer connects to the robot and the actuators in the supply unit via Ethernet and CAN.
- The computer loads geometry-file and a parameter-file into the bending program.
- The bending program executes the loaded bends with the loaded parameters and cuts the tape in the end.

In the presented work, additional functions are added:

- A new module for the automatic calibration of the heating parameters is added which can update the parameter-file regularly.
- A module for the automatic analysis of the remaining angle-error at the current heating parameters is implemented. The errors at different bending angles will be saved in an offset-table. With the knowledge of this error, corrections can be done to counterbalance the error.

The functionality of these two modules and the necessary tools are described in the following sections.

### 4. Measurement system for a control loop

In this section, the implementation of an optical measurement system is introduced. The system is integrated into the control loop and can automatically measure the shape parameters ( $l$ ,  $\alpha$ ,  $\beta$ ; see Fig. 2) of the manufactured UD-tape preforms. The measured geometry of the tapes are compared with the desired geometry. The manufacturing errors are calculated and used for process parameter optimization and are saved in an off-set table for automatic adaption of process parameters. To avoid influences of the current component shape, the process parameter and offset analysis is conducted on a standard specimen shape. This shape is manufactured by supplying a short strip of tape, bending and measuring it and then cutting it off. If longer strips were used, the geometry of the last bend would be influenced by the weight of the previous bends.

In order to design the above-mentioned measurement system, several sub-tasks are carried out subsequently: First, a measurement process is defined. Afterwards suitable hardware for the measurement is selected and commissioned in the demonstrator cell. In the next step, the resulting output of the

cameras is processed to calculate the manufacturing error. Using this, parameters in the manufacturing of the next parts can be adapted. Finally, the performance of the measurement system is evaluated.

#### 4.1. Control loop overview

The control architecture for performing the CFRP tapes is introduced in Section 3. In this section, a way of using the implemented functions to improve the bending accuracy is presented. The aim is to use the measurement system for experimentation on parameter calibration and offset-table generation. The whole control loop with a measurement process is shown in Fig. 5.

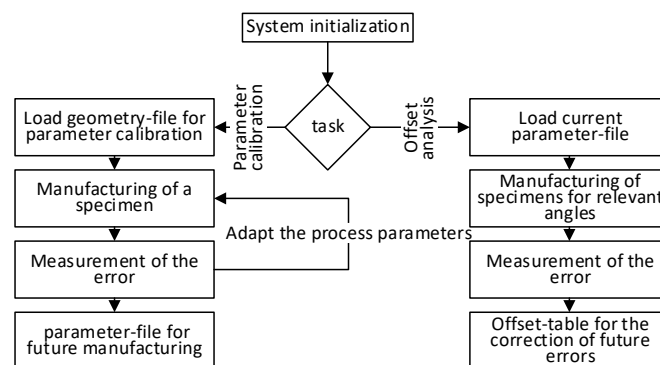


Fig. 5: Overview of the measurement process.

In order to simplify the measurement routine and improve the quality of the measurement, the standard specimen has only one bend and a short overall length. The reason for this is the flexibility of the tape which has increasing influence if the length of the tape is larger. On the standard one-bend-specimen, the rotational angle  $\alpha$  and the bending angle  $\beta$  of the tape are measured with only one bending process. The measured parameters of the tape are then saved into a list and used for parameter optimization.

#### 4.2. Hardware: camera and its integration in the robot cell

A suitable and robust camera system is selected and implemented in the robot cell. Due to the 3D geometry of the tape, a camera system which is capable of depth measurement should be chosen for the measurement task. Many approaches for 3D measurement are suitable for this task, such as triangulation, structured illumination, stereo image and time-of-flight sensors. Due to the limitation in space on the test site and for economic reason, a stereo vision system is chosen. Two webcams and an Intel RealSense D415 camera with an infrared emitter are tested for this task. Compared to other optical measurement systems the two above mentioned systems have following advantages: They are widely used in robotics with mature hardware and software, have acceptable depth resolution for this task, an RGB aligned depth image, quick capture and calculation of the depth image and a low-cost implementation [14]

In this work, the stereo vision is calibrated with the Matlab Toolbox „Stereo camera calibration app“ and calculates a

depth image with the OpenCV provided semi global block matching (SGBM) algorithm.

In the test, both systems provide similar result when the camera is placed 45° above and 2 meters away from the tape as in Fig. 6. The contour of the tape can be detected but the reflex of the surface of the tape, resulting from the lighting conditions in the test field, is destructive for the results of both optical systems. Thus, the depth resolution is reduced and holes on tape in depth image represent areas whose depth cannot be detected.

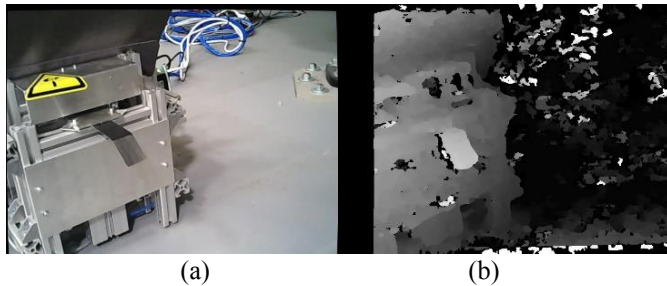


Fig. 6: RGB image (a) and aligned depth image (b) of tape with stereo vision. In the depth image, the contour of the supply unit is visible with noise in the background

For a better result of the depth image of the tape, the camera system is placed below the supply unit and can capture the tape through a mirror from the lower side. Thus, reflex is avoided and the camera can capture the tape with better resolution of depth information and without collisions with the robot arm in the manufacturing process. The flexibility of the algorithms of the stereo camera allows it to capture the tape in a distance of 500 mm, while the capture distance of the D415 camera is limited by Intel to larger than 160 mm theoretically, but on the test site the D415 only delivered a satisfactory depth quality of 0.002 m for objects located more than 1500 mm away. To minimize the influence of the lighting condition in the test site, a pneumatically driven metal cover is built onto the supply unit, which is moved forward to cover the tape from the windows and lights during measurement. The picture is now taken from the lower side of the tape (Fig. 7 (a)). The result of the depth image of the camera integrated in the robot cell is shown in Fig. 7 (b). The depth information on the tape is accurate and continuous. The noises in the background or foreground is caused by the stereo algorithm with a limited capture range but do not affect the result. Thus, the tape is very well distinguished from the background.

#### 4.3. Measurement program with machine vision algorithms

The measurement program is implemented with machine vision algorithms from the open-source library OpenCV. The image will be processed in the following steps:

- Capturing of an image (Fig. 7 (a,b))
- Segmentation of the image to isolate the tape (Fig. 7 (c))
- Creation of a point cloud of the tape (Fig. 7 (d))
- Segmentation of the tape at the bend line
- Calculation of the planes of the tape (Fig. 9)
- Calculation of  $\alpha$  and  $\beta$

Firstly, the left and right RGB images of stereo cameras are rectified with stereo calibration parameters and converted to

grayscale for depth image calculation. With the depth image, some pixels are segmented with a combination of two thresholds: Pixels with gray value smaller than 40 and distance smaller than 550 mm. Then, a mask with the largest area is the contour of the tape as in Fig. 7 (c). The points on the tape are smoothed with a median filter and stored as a point cloud (Fig. 7 (d)) with color and depth information. Afterwards, the points are distributed to two planes. The normal of the two planes are calculated with a 3D RANSAC or Minimum Square Method. With both normals of the planes, the rotational angle  $\alpha$  and bending angle  $\beta$  can be calculated using the cross product.

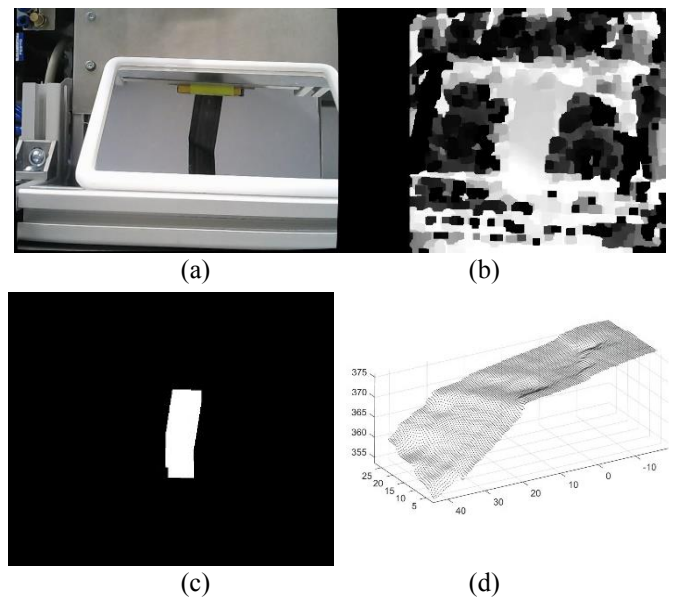


Fig. 7: 30mm wide UD-tape: RGB image (a), depth image (b), segmented image (c) and point cloud (d) of the tape from the stereo camera with a mirror

In this work, some approaches for distributing the points on the tape into two subsets for the two planes (one on each side of the bend) are implemented and tested. Table 2 gives an overview over the methods.

Table 2 Methods for distributing points into two planes.

Method	Description
Gradient in depth on sloping plane	Calculate depth changes (gradients) with a canny edge detector on sloping planes
Reference depth for the horizontal plane	Use depth of a sticker on the supply unit as reference depth threshold
3D Hough transformation	Calculate normal of single point with its neighborhood and find 2 major clusters of normals [15]
Iterative distributing of points and calculating of the normal	Plane fitting for 2 subsets with iteratively distributed points, use point distribution with the minimum error

In the test, the iterative distributing of points and calculating of the normal is most stable and delivers the best results for the overall measurement error. This procedure works as following: First, the point cloud is segmented into groups of points depending on their distance to the supply unit. In the next step, a plane is fitted to the first group. The normalized error of the fitting is then calculated and saved. After the next group of points has been added, a new plane is fitted and the normalized

error of the fitting is saved. An example for the error values is presented in Fig. 8. As long as the added points are on the same side of the bend, the error will decrease. As soon as point on the other side are added it is no longer possible to properly fit a plane and the error will increase. The iteration with the minimal error is used to set the divider in the point cloud for the angle calculation.

Once the point cloud is distributed onto the two halves of the tape, the planes of the tape (Fig. 9) and thus the geometry of the bend can be calculated. To do this, planes are fitted to the two remaining groups of points. After these planes are calculated, the direction and amount of bending and the direction of the bending line can be calculated using the cross product between the normalized normal vectors of the planes.

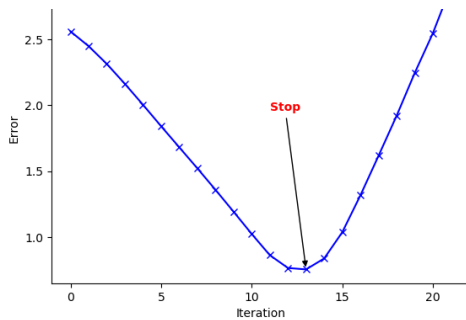


Fig. 8: Normalized error for iteratively plane fitting

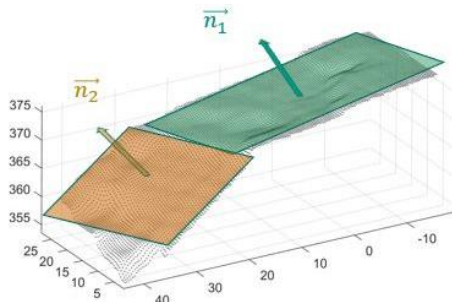


Fig. 9: Two planes fitted to the point cloud (axes in mm)

#### 4.4 Evaluation of the measurement system

For the test tapes with a rotational angle  $\alpha$  of  $10^\circ$  and different bending angles  $\beta$  from  $-70^\circ$  to  $60^\circ$  (interval of  $10^\circ$ ), the measurement error is measured multiple times. A measure error off less than  $2^\circ$  for the  $\beta$  angle is achieved compared to a measurement with a traditional angle meter (Table 3). Due to the elasticity of the CFRP tapes, this result in the precision range of the traditional angle meter is acceptable. The best measurement precision appears for  $|\beta|$  in  $40^\circ$  to  $60^\circ$ , because in this range of  $|\beta|$  the tape has a relatively large area of projection containing more points than tapes with  $|\beta|$  larger than  $70^\circ$ . Due to the lack of obvious depth changes on tapes with  $|\beta|$  smaller than  $20^\circ$ , errors are caused because the algorithm cannot reliably segment the tape into its both ends and large deviations occur. Therefore, results with  $|\beta|$  smaller than  $20^\circ$  might be discarded. Results could be further improved by pattern projection. Due to the limitation of the SGBM algorithm, the calculated point cloud as in Fig. 7(d) is in a step shape, which disturbs the result of the plane fitting. [16] In this work a  $3 \times 3 \times 3$  median filter for the point cloud is used to improve this.

Table 3: Actual value and average measured value of bending angle  $\beta$ :

Actual Value	$-70^\circ$ $-60^\circ$ $-50^\circ$ $-40^\circ$ $-30^\circ$ $-20^\circ$ $-10^\circ$ $10^\circ$ $20^\circ$ $30^\circ$ $40^\circ$ $50^\circ$ $60^\circ$
Measured Value	$-67^\circ$ $-60^\circ$ $-50^\circ$ $-39^\circ$ $-29^\circ$ $-22^\circ$ $0^\circ$ $0^\circ$ $19^\circ$ $30^\circ$ $40^\circ$ $51^\circ$ $58^\circ$

## 5 Automated adaption of bending process parameters

A major problem in manufacturing CFRP tapes is to determine the correct process parameters, such as heating and preheating time. Before the manufacturing process with a given material, the process parameters should be adapted to this material. The manual adaption of these parameters can be very time consuming. Therefore, an automated adaption of process parameters using the measurement system is implemented.

The following process can be used to improve an already working parameter set. It could for example optimize the single parameters sequentially at the beginning of a manufacturing shift. The process for the optimization of a single parameter carries out an automatic iteration of this parameter while bending and measuring the tape.

The program varies the parameter (in the described example the heating time) in a certain range. After this process, a correct time can be read from the .txt-file storing the used time and the resulting geometry (here:  $\beta$ ) with this parameter. This can either be done by picking the heating time with lowest deviation or by applying a function to find a compromise between deviation and process time. An example process with coarse time steps for demonstration of the adaption of the heating time is shown in table 4.

Table 4: Adaption of the heating time with a preheating time of 3.0s and  $\beta = -45^\circ$ .

Heating time	0 s	0.5 s	1.0 s	1.5 s	2.0 s	2.5 s
Measured Value of $\beta$	$-36^\circ$	$-37^\circ$	$-41^\circ$	$-43^\circ$	$-45^\circ$	$-45^\circ$

If completely new parameters have to be found, the measurement system can be used to create an overview over working parameters. For this, it will be programmed to execute experimental plans which would be very time-consuming to do manually. Any suitable experimental plans can be executed for process examination in research. One example is the combined variation of preheating and heating time as shown in Table 5. As the test rig was re-adjusted between the experiments and the environmental conditions changed, the values are not comparable to Table 4.

Table 5: Combined variation of preheating and heating time for  $\beta = -30^\circ$  and  $\beta = -45^\circ$ :

		$\beta = -30^\circ$ : heating				$\beta = -45^\circ$ : heating			
		0 s	1 s	2 s	3 s	0 s	1 s	2 s	3 s
preheating	1 s	$0^\circ$	$0^\circ$	$-22^\circ$	$-23^\circ$	$0^\circ$	$-0^\circ$	$-39^\circ$	$-40^\circ$
	2 s	$0^\circ$	$-24^\circ$	$-28^\circ$	$-26^\circ$	$0^\circ$	$-37^\circ$	$-35^\circ$	$-41^\circ$
	3 s	$-24^\circ$	$-28^\circ$	$-28^\circ$	$-28^\circ$	$-34^\circ$	$-40^\circ$	$-42^\circ$	$-43^\circ$

The second functionality of the measurement system is the generation of an offset table for error correction. It can be used when materials are processed which cause larger manufacturing errors. To generate such an offset table, bending

experiments will be conducted with a variety of desired angles and the resulting measured angles are saved. In the future production with the used material, the offset table can be used to deliberately increase the bending angle if the manufacturing error is towards smaller angles and vice versa. The method is described on one example angle below (see Table 6). First, specimens are manufactured with a desired  $\beta = -45^\circ$  (Calculation run C1, C2 and C3). The average measured  $\beta$  outcome is  $\beta = -42.1^\circ$ . The actual bend of the tapes is therefore  $2.9^\circ$  less than the desired bend. To correct the error, future specimens are manufactured with  $\beta = -48^\circ$  (approximately the sum of desired angle and error) to obtain a resulting  $\beta = -45^\circ$ . The result is presented in the Columns V1-V3 /Validation 1-3) in Table 6.

Table 6: Correction of a  $\beta = -45^\circ$  bend.

	C1	C2	C3	V1	V2	V3
Desired/corrected $\beta$		$-45^\circ$			$-48^\circ$	
measured $\beta$	$-41.4^\circ$	$-41.5^\circ$	$-43.2^\circ$	$-47.9$	$-44.1$	$-43.6$
average $\beta$		$-42.1^\circ$			$-45.2$	
Error to $\beta = 45^\circ$		$-2.9$			$0.2$	

To use this approach in manufacturing, a wider range of angles has to be corrected. For this, several angles are measured as fulcrums and values in between are interpolated. The initial manufacturing error and the error after the described correction is shown in Fig. 10. To derive these values, the average of five experiments was used. Only values with an error larger than  $1.5^\circ$  were corrected. The results make apparent, that correction needs to be conducted carefully to avoid overshooting if the exemplary process showed unusually strong error.

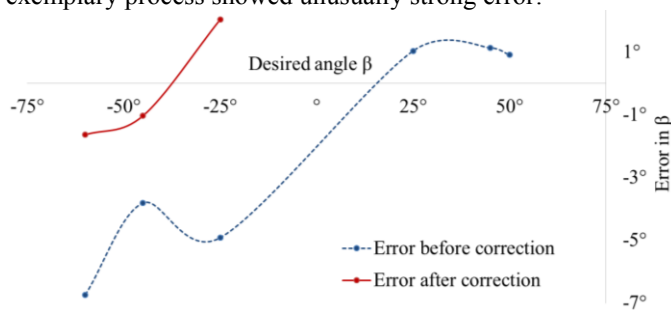


Fig. 10: Improvement of the bending error in the negative  $\beta$  region

## 5. Summary and Outlook

The bending process for the iterative preforming of UD-tape has been presented in this paper. Research has already been done in the fields of the adaption to manufacturing constraints and process parameter optimization. In the previous work it became apparent, that new materials and changed environmental conditions would require adapted process parameters for the single bends on the tape. As the adaption is a time consuming manual process, a solution for its automation had to be found. The chosen approach uses a standardized measurement cycle, in which a stereo camera system measures the result of the process. This is compared with the desired result. Now, either the process parameters can be changed to improve the future manufacturing, or the error can be saved to correct the future manufacturing with an offset. This can increase the precision of the preforming process significantly,

while decrease the amount of manual work for running the cell in industry. In research, the automated measurement will be used for larger parameter studies which could not be conducted without it due to the high number of parameters. It is expected, that the digital process management will indirectly improve the understanding of the process this way.

Apart from parameter studies, the preforming process will be extended by a joining station. It will be used to assemble the single preforms to reinforcement structures as shown in Fig. 1. These assembled reinforcement structures are the basis for the co-molding with a flowable mass to manufacture finished components.

## Acknowledgement

The research documented in this manuscript has been funded by the German Research Foundation (DFG) within the International Research Training Group “Integrated engineering of continuous-discontinuous long fiber reinforced polymer structures” (GRK 2078). The support by the German Research Foundation (DFG) is gratefully acknowledged.

## References

- [1] Lamontia, M., Funck, S.B., Gruber, M.B., Cope, R.D. et al., 2003. Manufacturing flat and cylindrical laminates and built up structure using automated thermoplastic tape laying, fiber placement, and filament winding, p. 30.
- [2] Olsen, H.B., Craig, J.J., 1993. Automated composite tape lay-up using robotic devices, p. 291.
- [3] Behrens, B.-A., Raatz, A., Hübner, S., Bonk, C. et al., 2017. Automated Stamp Forming of Continuous Fiber Reinforced Thermoplastics for Complex Shell Geometries 66, p. 113.
- [4] Brecher, C., Emonts, M., Ozolin, B., Schares, R., 2013. Handling of Preforms and Prepregs for Mass Production of Composites, in *The 19th international conference on composite materials*.
- [5] Kordi, M.T., Hüsing, M., Corves, B., 2007. *Development of a Multifunctional Robot Endeffector System for Automated Manufacture of Textile Preforms: 4 - 7 Sept. 2007, Zurich, Switzerland*. IEEE Service Center, Piscataway, NJ.
- [6] Förster, F., Ballier, F., Coutandin, S., Defranceski, A. et al., 2017. Manufacturing of Textile Preforms with an Intelligent Draping and Gripping System 66, p. 39.
- [7] Kupzik, D. Flexible preforming of CFRP by robot based bending. <https://youtu.be/HjTxdq9gwqM>. Accessed 2 May 2019.
- [8] Luhmann, T., 2010. Close range photogrammetry for industrial applications, in *ISPRS Journal of Photogrammetry and Remote Sensing*, p. 558.
- [9] Uffenkamp, V., 1993. State of the Art of High Precision Industrial Photogrammetry, in *Proceedings, 3rd International Workshop on Accelerator*, Annecy, France, II153-II164.
- [10] Farnood Ahmadi, F., 2017. Integration of industrial videogrammetry and artificial neural networks for monitoring and modeling the deformation or displacement of structures 28, p. 3709.
- [11] Huang, Q.S., Luan, H., Jin, Y. Systems and Methods for Compensating for 3D Shape Deviations in Additive Manufacturing, 2016(US 10,474,134, B2). Accessed 13 January 2020.
- [12] Kupzik, D., Coutandin, S., Fleischer, J., 2019. Toolless Forming for Load-adapted UD Reinforcements 12, p. 38.
- [13] Kupzik, D., Biergans, L., Coutandin, S., Fleischer, J. Kinematic Description and Shape Optimization of UD-Tape Reinforcements Manufactured with a Novel Preforming Process, in *Procedia Cirp*, p. 78.
- [14] Beyerer, J., Puente León, F., Frese, C., 2016. *Machine Vision: Automated Visual Inspection: Theory, Practice and Applications*, 1st edn. Springer Berlin Heidelberg, Berlin, Heidelberg.
- [15] Borrmann, D., Elseberg, J., Lingemann, K., Nüchter, A., 2011. The 3D Hough Transform for plane detection in point clouds: A review and a new accumulator design 2, p. 381.
- [16] Kaehler, A., Bradski, G., 2016. *Learning OpenCV 3*. O'Reilly Media.